Forming self-rotating pinwheels from assemblies of oscillating polymer gels

Debabrata Deb[1], Olga Kuksenok[1] , Pratyush Dayal[1,2], and Anna C. Balazs[1*]

[1] Chemical Engineering Department, University of Pittsburgh, Pittsburgh, PA 15261

[2]Present address: Department of Chemical Engineering, Indian Institute of Technology, Gandhinagar 382424, India

Supporting Information

A. Model parameters and their relationship to experimental values

Where possible, our model parameters were taken from known experimental data. In particular, for the BZ reaction parameters, we set [1, 2] $\varepsilon = 0.12$, $f = 0.9$ and $q = 9.52\times10^{-5}$ and for the parameters characterizing the properties of the gel, we set $\phi_0 = 0.139$, and $c_0 = 1.3\times10^{-3}$ (based on experimental data provided in ref. [3]). For the gel-solvent interaction parameters, we used $\chi_0 = 0.338$ and $\chi_1 = 0.518$, which correspond to the NIPAAm gel-solvent interaction parameters at $20^0 C$ for a gel with the above values of ϕ_0 and c_0.[4] We also set $\chi^* = 0.105$; χ^* is an adjustable parameter of the model and is chosen to have the same value as in refs. [1, 5-9].

For the initial conditions within the gels, we chose the concentrations of the oxidized catalyst and activator to be randomly distributed around their stationary solutions for the given reaction parameters,[10] $v_{st} = 0.089$ and $u_{st} = 0.093$. Specifically, a random noise is initially added to these values of v_{st} and u_{st}; the amplitude of the noise is 20% of the latter values. In addition, we set the initial degree of swelling λ to its stationary value $\lambda_{st} = 1.48$.

To determine the characteristic length and time scales of the system, we assume that the diffusion coefficient of the activator, $D_u = 2\times10^{-9}\ m^2/s$, remains the same in the gel and surrounding fluid.[11] Using the above values, we find our dimensionless units of time and length

correspond to the respective physical values of $T_0 \approx 0.31\ s$ and $L_0 = \sqrt{D_u T_0} \approx 25 \mu m$.[12] Hence, the initial dimensionless length of a cubic sample, $l = 8.9$, corresponds to ~0.22 *mm*. Finally, we use the same parameters for short-range repulsion between the gel as defined in ref.[12] , with the value of the cut-off distance for this inter-gel interaction fixed at $r_c = 1.5$ units.[12]

In our simulations, the dimensionless velocity of the gel's expansion/contraction is approximately 0.1, which corresponds to $v \sim 8 \mu m/s$. If hydrodynamic effects were taken into account, then it would be reasonable to assume that the characteristic velocities created by these oscillating gels within the fluid would be of the same order of magnitude as v, which would yield a low Reynolds numbers of $Re = (\rho v\ l / \mu) \sim 2 \times 10^{-3}$ (using the dynamic viscosity μ and density ρ of water, and taking the characteristic length scale to be the linear dimension of the gel, $l = 0.22mm$). Additionally, the hydrodynamic forces acting from the fluid on the gel's surface would be negligibly small [8] due to the low ratio of the viscous to elastic forces; this ratio, which represents the capillary number, [13] can be estimated as $Ca = v \mu / l K \sim 3 \cdot 10^{-10}$, where the elastic modulus of the NIPAAM gel is taken to be $K = 10^5 Pa$.[4] Hence, due to the slow dynamics of the gels and the low viscous forces, we can neglect hydrodynamic effects .[8]

B. Additional figures

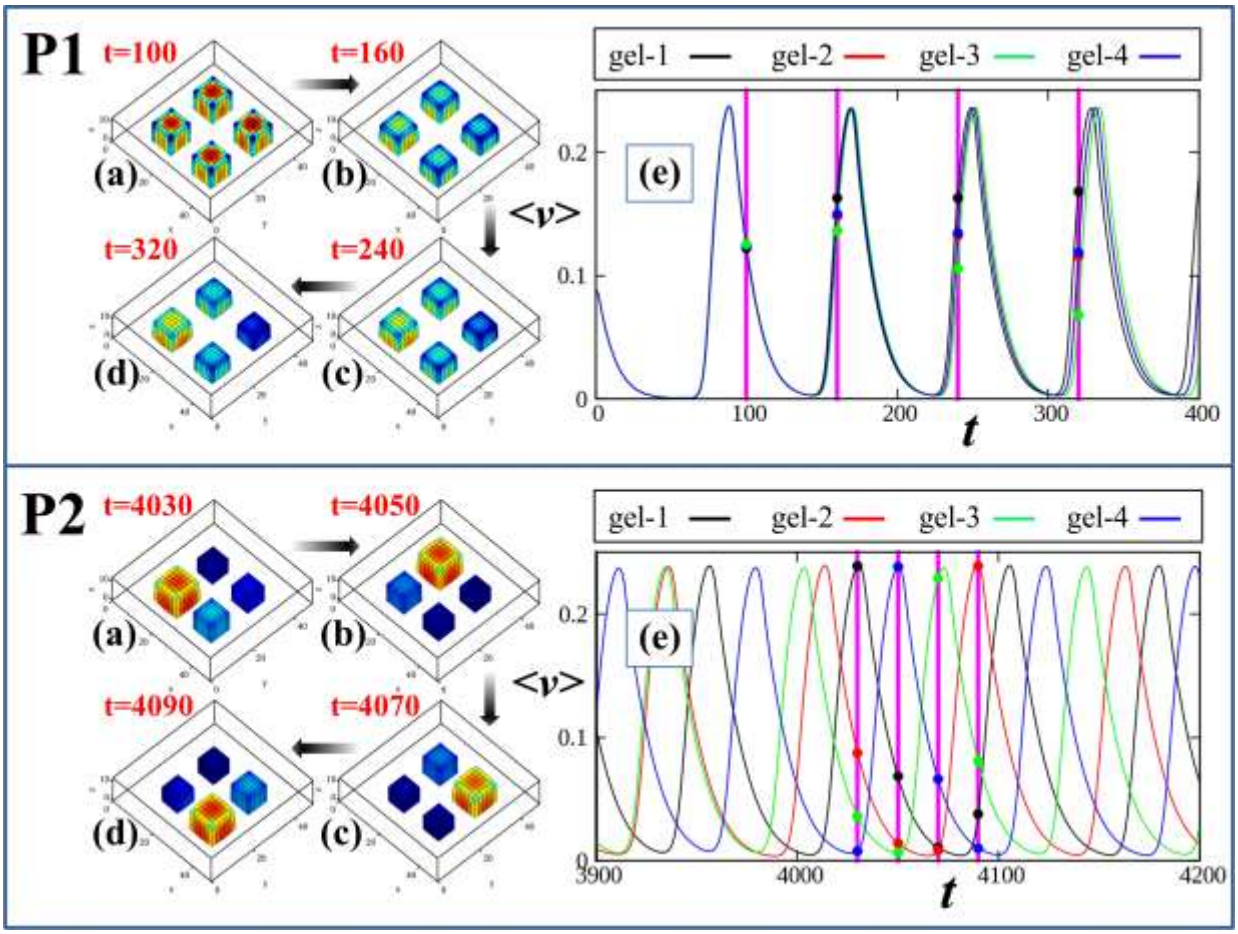

Figure S1. **Phase-locking of chemo-mechanical oscillations in the gels. In P1,** the snapshots (a), (b), (c) and (d) show the gels at early times *t=100, 160, 240 and 320*, respectively. (e) Evolution of the average concentration of oxidized catalyst, <*v*>, in each gel. The vertical magenta lines are positioned at times that correspond to the snapshots on the left. The filled circles on these lines mark the values of <*v*> in the four gels. Initially, the chemo-mechanical oscillations in the gels are synchronized (see snapshot (a) and the position of the filled points in (e) at *t*=110). Immediately after a few oscillations, however, we observe desynchronization in the

gels oscillations, which is evident from the increased spread among the points on the vertical lines at *t=160, 240 and 320*. **In P2,** the snapshots (a), (b), (c) and (d) show the gels at times *t=4030, 4050, 4070* and *4090*, respectively. (e) Evolution of the average concentration of oxidized catalyst, <*v*>, in each gel. In contrast to the snapshots in P1, the snapshots in P2 show that the oscillations in the gels are now again synchronized, exhibiting a constant phase difference between neighboring pairs and hence, the oscillations are phase-locked. In phase-locked system, the oscillations propagate either in a clockwise direction (as shown here) or in a counter-clockwise direction. (Note that for each gel, the values of <*v*> on the vertical lines in P2e show a systematic pattern with time, reflecting the cyclic changes in this parameter as the oscillations propagate from neighbor to neighbor in a clockwise direction.) For gel numbering in P1 and P2, see Fig. S2.

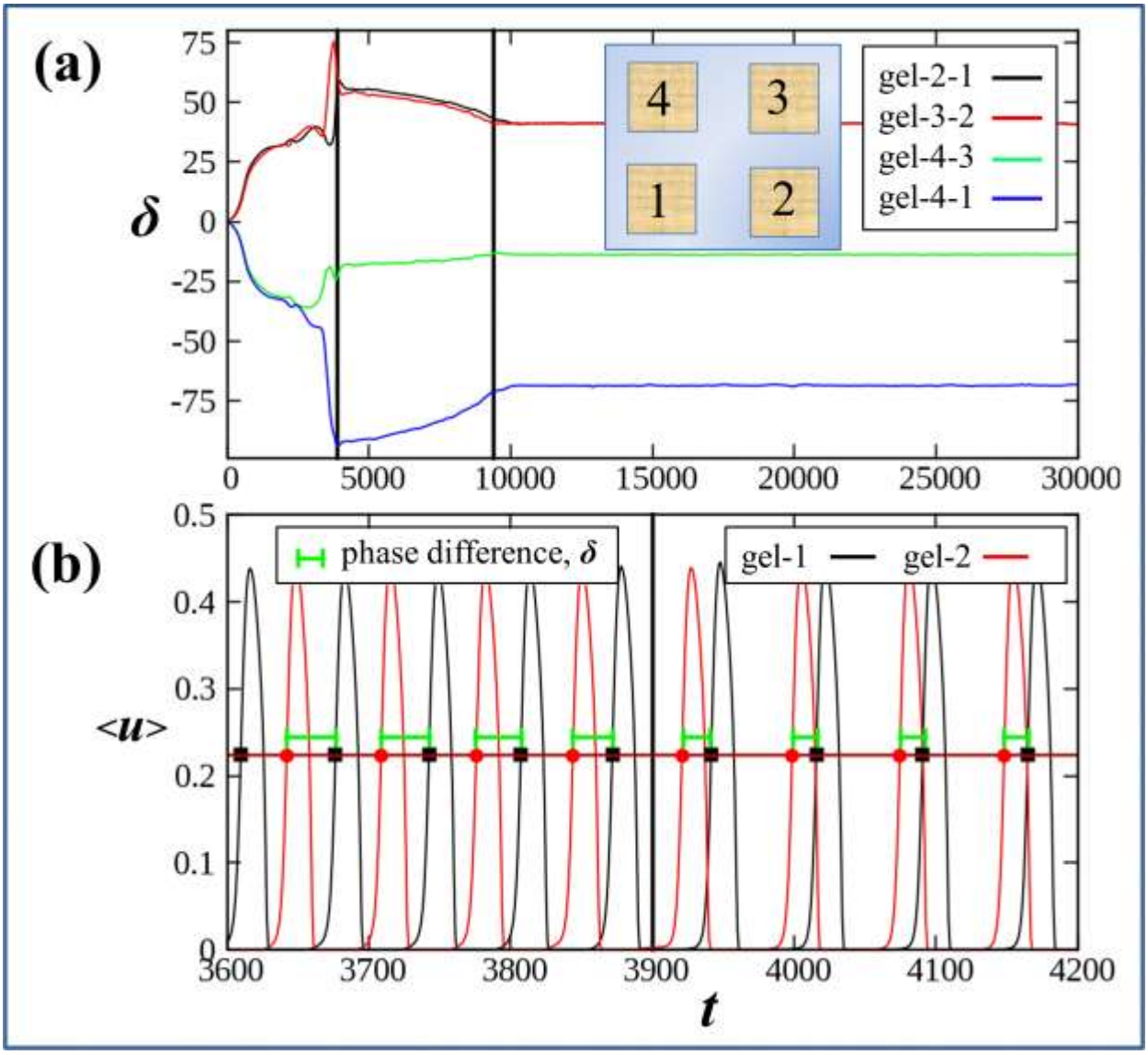

Figure S2. **(a). Time evolution of the phase difference, δ**, calculated from the oscillations in the average activator concentration $\langle u \rangle$ between two neighboring gels. The vertical black lines are positioned at *t=3900* and *9400*. For *t>3900,* δ changes very slowly and after *t=9400*, it remains constant. **The value of δ is calculated as shown in (b)**, where $\langle u \rangle$ is plotted versus time for gel-1 (black curve) and gel-2 (red curve). A pair of consecutive black squares (or red circles) marked on the black (or red) curve identifies one period of oscillation of $\langle u \rangle$ in gel-1 (or gel-2) and the difference between a pair of black and red symbols (marked by a green bar) is the

phase difference δ corresponding to that moment in time. We identify here the moment when the phase locking occurs to be at $t=3900$ as after this, δ changes very slowly with time. This slow change is due to the gels continuing movement towards each other and the center of the box (see for example, Fig. S3, which clearly illustrates that the distance between the gels continue to decrease during the timeframe $3900<t<9400)$. The value of δ remains constant after $t=9400$ because after this time, excluded volume interactions between neighboring gels begin to influence the dynamics and correspondingly, the motion of the gels towards each other and the center of the box is no longer observed (see Fig. S3).

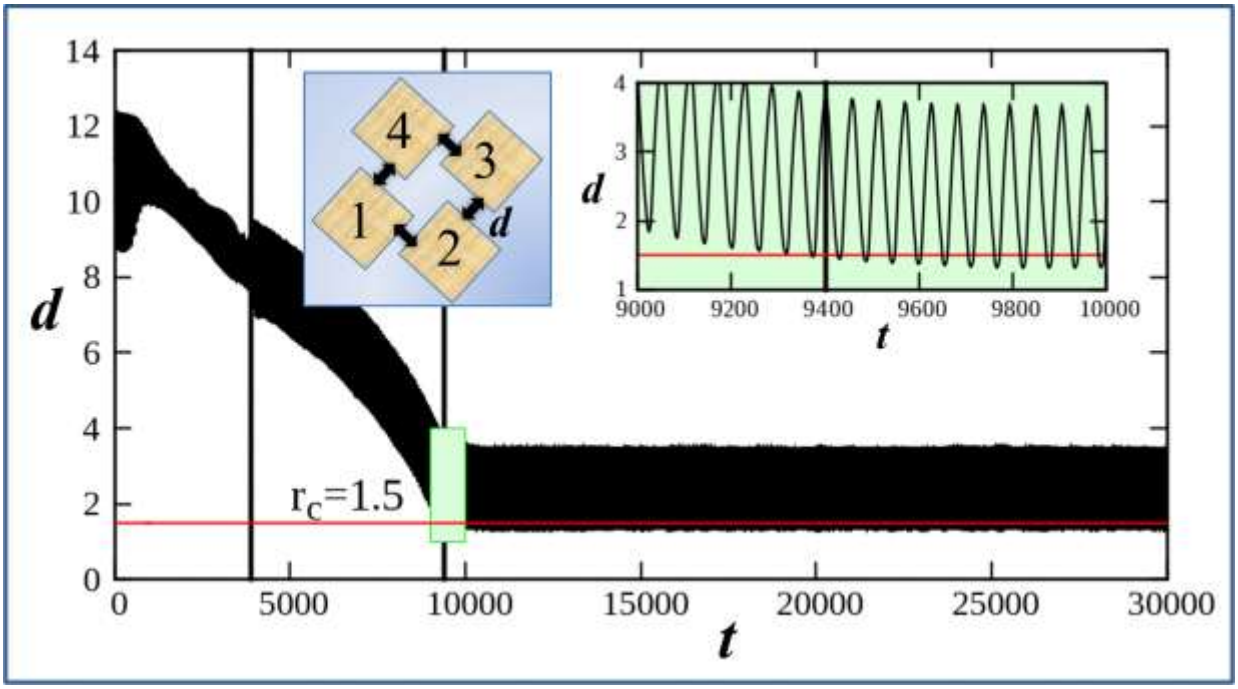

Figure S3. **Evolution of the separation *d* between the faces of two neighboring gels numbered 1 and 2.** The inset on the left shows a schematic of the four gels. The value of *d* oscillates with time because the gels undergo periodic swelling and deswelling. The vertical black lines are positioned at *t=3900* and *9400*. At *t=3900*, the phase locking occurs as explained in Fig S2. At *t=9400*, the minimum of *d* reaches the critical distance r_c*=1.5*, and excluded volume interactions between neighboring gels begin to influence their dynamics. The portion of the curve under the light green rectangle is shown in the inset on the right; the vertical black line at *t=9400* marks the time at the middle of the first oscillation period when the distance between the gel faces reaches r_c for the first time. By comparing this plot with the plot in Fig. 2a, we can clearly see that the moment in time when *d* reaches the critical distance r_c (t=9400) corresponds to the moment in time when the individual gels begin to rotate (see green line in Fig. 2a); i.e., to the moment of pinwheel formation. For clarity, we plot only the distance between the faces of

gels 1 and 2; all four gels do, however, come into close contact within a few cycle of oscillations after the latter gels (data are not shown).

References

1. V. V. Yashin and A. C. Balazs, *J Chem Phys*, 2007, **126**, 124707.
2. O. Kuksenok, V. V. Yashin, M. Kinoshita, T. Sakai, R. Yoshida and A. C. Balazs, *Journal of Materials Chemistry*, 2011, **21**, 8360-8371.
3. S. Sasaki, S. Koga, R. Yoshida and T. Yamaguchi, *Langmuir*, 2003, **19**, 5595-5600.
4. S. Hirotsu, *J Chem Phys*, 1991, **94**, 3949-3957.
5. V. V. Yashin and A. C. Balazs, *Science*, 2006, **314**, 798-801.
6. P. Dayal, O. Kuksenok and A. C. Balazs, *Langmuir*, 2009, **25**, 4298-4301.
7. P. Dayal, O. Kuksenok and A. C. Balazs, *Soft Matter*, 2010, **6**, 768-773.
8. P. Dayal, O. Kuksenok, A. Bhattacharya and A. C. Balazs, *J Mater Chem*, 2012, **22**, 241-250.
9. V. V. Yashin, O. Kuksenok, P. Dayal and A. C. Balazs, *Reports on progress in physics*, 2012, **75**, 066601.
10. O. Kuksenok, V. V. Yashin and A. C. Balazs, *Phys Rev E*, 2008, **78**, 041406.
11. R. Yoshida, G. Otoshi, T. Yamaguchi and E. Kokufuta, *J Phys Chem A*, 2001, **105**, 3667-3672.
12. P. Dayal, O. Kuksenok and A. C. Balazs, *PNAS*, 2013, doi: 10.1073/pnas.1213432110
13. A. Bhattacharya and A. C. Balazs, *J Mater Chem*, 2010, **20**, 10384-10396.